Metal Ion Exchange in Zn-Dependent S1 Nuclease: Effect on the Structure

Jakub Hrubý [1,2⋆], Petr Kolenko [1,2], Tomáš Koval' [2], Kristýna Adámková [2,3], Blanka Husťáková [2,3], Lars H. Østergaard [4], Jan Dohnálek [2⋆]

[1] Dept. of Solid State Engineering, Faculty of Nuclear Sciences and Physical Engineering, Czech Technical University in Prague,
[2] Institute of Biotechnology of the Czech Academy of Sciences, v.v.i.,
[3] Dept. of Biochemistry and Microbiology, University of Chemistry and Technology Prague,
[4] Dept. of Agile Protein Screening, Novozymes A/S, Denmark
⋆ Corresponding authors; hrubyj18@fjfi.cvut.cz (JH), jan.dohnalek@ibt.cas.cz (JD)

Abstract

S1 nuclease is an enzyme commonly used in biotechnology applications. Its activity depends on the presence of three Zn^{2+} ions in the active site. In this work, we examine the possibility of exchanging natively present Zn^{2+} ions with Cd^{2+}. EDTA-treated S1 nuclease was successfully crystallised in the presence of $CdCl_2$. The anomalous signal from three different energies confirmed the exchange of two Zn^{2+} ions to Cd^{2+}. The residues of the active site remained structurally conserved.

Keywords: nuclease; protein crystallography; X-ray structure analysis; metalloenzymes; metal ion exchange; anomalous signal.

Introduction

Nucleases constitute an essential class of enzymes. They are capable of cleaving phosphodiester bonds in nucleic acids. S1 nuclease from the S1-P1 family of nucleases is a metalloenzyme that contains three zinc ions in its active site [1]. It consists of approximately 270 amino acids with a molecular weight reaching 30 kDa. [2]. Its secondary structure is formed of α-helices with the addition of two short β strands (Fig. 1). The zinc cluster is located in a pocket; two positions of ions (designated *M 1* and *M 2*) are buried at the bottom, while the third (*Zn 3*) is closer to the surface of the nuclease. In total, nine amino acid residues coordinate the zinc cluster. The cluster and its adjacent residues are conserved across the entire S1-P1 family of nucleases.

In the case of S1 nuclease, a strong preference towards single-stranded nucleic acids (ssNA) is observed [2]. This can be used in the analysis of transcription and translation sites. The optimal pH for the activity of S1 nuclease is significantly acidic (pH 4 – 4.3).

The activity of S1 nuclease depends on the presence of zinc ions in the active site. According to Gite and Shankar [3], the removal of one Zn^{2+} ion using the chelating agent ethylenediaminetetraacetic acid (EDTA) results in a significant loss of activity (EDTA-treated S1 shows only about 50% activity compared to native S1). The removal of two or three Zn^{2+} ions results in a complete and irreversible loss of activity, most likely due to the disruption of the secondary structure [3].

To date, it has been unclear whether it is possible to exchange metal ions at the active site of the nuclease and whether the exchange has an effect on the structure of the nuclease. This observation can be made using X-ray anomalous dispersion (XAD) [4]. In this work, our objective is to show that the exchange of zinc ions, natively present in the active site of S1 nuclease, to cadmium ions is possible. We present diffraction data collected at three different X-ray energies together with the anomalous maps. We analyse the effect of ion exchange on the structure of the active site.

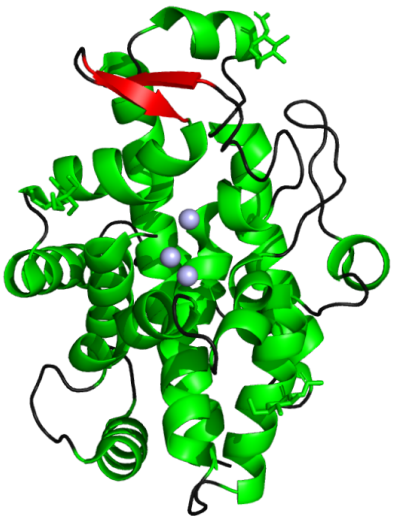

Figure 1: S1 nuclease (PDB ID 5FB9) in secondary structure representation. Zinc atoms are represented as light blue spheres. Molecular graphics created using PyMOL.

Materials and Methods

S1 nuclease from *Aspergillus oryzae* provided by Novozymes A/S was deglycosylated using 1 μl of endoglycosidase Endo-F1 (17 U·ml^{-1}, Sigma-Aldrich) per 1 mg of enzyme in a reaction buffer (1mM $ZnCl_2$, 100 mM sodium acetate pH 4.6) for 120 minutes at 37°C.

The EDTA-treatment consisted of mixing EDTA (at a stock concentration of 3.3 mM) with S1 in storage buffer (50 mM NaCl, 25 mM Bis-Tris, pH 6.0) to reach the 5:1 molar ratio, respectively. The solution was incubated at room temperature for 120 minutes. Subsequently, the solution was dialysed against 1000 ml of storage buffer for 16 hours. After dialysis, EDTA-treated S1 (ES1) was stored at a concentration of 5.8 mg·ml^{-1} in 4°C. The concentration was measured using DeNovix DS-11 FX+ nanodrop spectrophotometer at 280 nm. ES1 was then mixed with $CdCl_2$ to reach a 1:10 molar ratio, respectively, and a final protein concentration of 5.5 mg·ml^{-1}.

Crystallisation was performed using the vapour diffusion method in the hanging drop configuration at 20°C. 1 ml of 25% polyethyleneglycol 3350, 200 mM NaCl, 50 mM $CaCl_2$, and 100 mM Bis-Tris pH 5.5 was used as a reservoir solution. The drop consisted of 1 μl of the reservoir solution and 2 μ l of the ES1 and $CdCl_2$ solution (in a 1:10 molar ratio). Obtained crystals were cryoprotected in perfluoropolyether, fished out of the drop using a kapton loop, and flash frozen in liquid nitrogen.

The diffraction experiment was carried out at the Bessy II synchrotron radiation source, Helmholtz Zentrum Berlin (HZB) [5], BL 14.1. X-ray energies for the diffraction experiment were chosen as follows: Cd-peak energy was chosen as the lowest experimentally possible energy (6 600 eV) with regard to the technical parameters of the beamline and air scattering. Zn-low and Zn-peak energies were selected to be slightly lower and higher than the Zn absorption edge energy (see Tab. 1). In total, three data sets with an oscillation angle total of 720° each were collected, as the objective was to obtain satisfactory multiplicity and completeness.

The data sets were integrated and scaled using XDS [6] and AIMLESS [7] software. Selected statistics of the data processing are presented in the Tab. 1. Subsequently, the structure was solved by molecular replacement in Phaser [8]. The structure of S1 (PDB

ID 5FB9, [1, 9]) with manually deleted Zn ions was used as an input model for the search. Refinement was performed using Refmac5 [10] with 5% of the total number of reflections set apart to form the Free set. Manual inspection of the structure was done in Coot [11].

Results

Crystallisation of ES1 and $CdCl_2$ solution was successful and provided crystals of sufficient quality and size. However, the incidence of visual defects was almost permanent and there was little improvement after optimisation. The diffraction data was collected using a single crystal segment that diffracted up to 2.3 Å.

Data processing showed satisfactory values for data collection statistics (Tab. 1). Two molecules in the asymmetric unit were found in the molecular replacement. The refined electron density provided the details expected at this resolution.

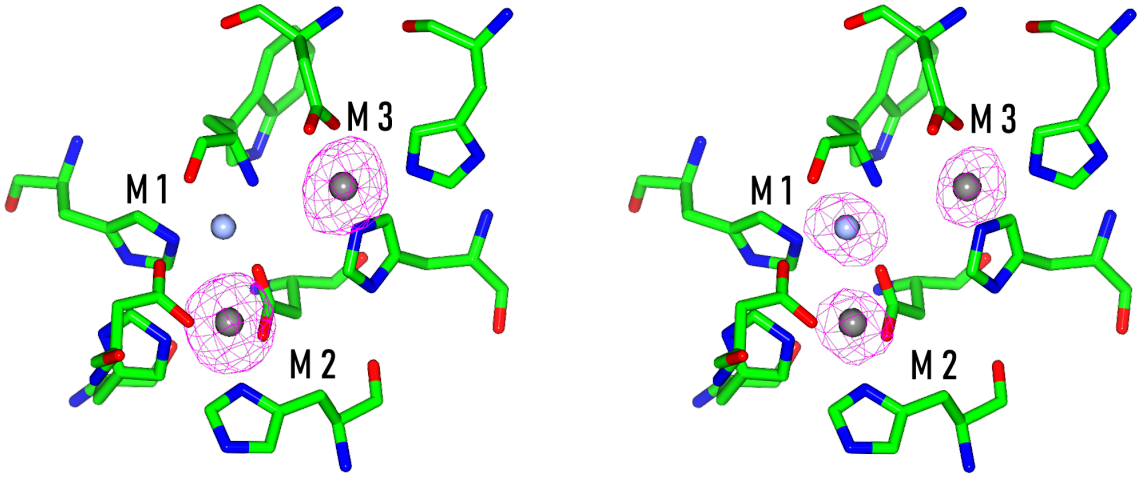

Figure 2: Anomalous difference maps at a level 5 σ (Cd-peak left, Zn-peak right) represented by a magenta mesh. Cd^{2+} and Zn^{2+} ions are shown using grey and light blue balls, respectively. Graphics generated using CCP4mg [12].

The anomalous signal measured at three different wavelengths was sufficient to obtain convincing anomalous difference maps. The anomalous maps are shown in Fig. 2. The maxima of the peaks are shown in Tab. 1. The Cd-peak data set shows two strong anomalous peaks at the positions *M 2* and *M 3*. The Zn-low data set shows peaks at the same positions as the Cd-peak, albeit weaker. Finally, the Zn-peak data set shows an anomalous signal at all three positions. Compared to the previous two data sets, a significant increase of the anomalous signal is observed at the position *M 1*.

Apart from the possible exchange of metal ions that will be discussed later, no further changes in the surrounding amino acid residues were observed.

Discussion

Measurement of the anomalous signal serves as an indicator of the successful exchange of metal ions. However, it is not possible to determine the exact fraction of the molecules

where the exchange occurred using X-ray diffraction, as the anomalous signal is obtained as an average of a large number of molecules present in the crystal lattice.

The position *M 1* shows a negligible anomalous signal at Cd-peak and Zn-low energies. However, a significant increase of the anomalous signal between the Zn-low and Zn-peak data sets proves the presence of Zn^{2+} at this position.

Concerning the metal ion positions *M 2* and *M 3* first, the anomalous map maxima at Cd-peak energy prove the presence of Cd^{2+} at these positions. The decrease of the anomalous signal between Cd-peak and Zn-low energy is consistent with the theory of anomalous diffraction.

Apart from the exchange of Zn^{2+} to Cd^{2+} at positions *M 2* and *M 3*, no other changes were observed in the structure of the active site. The surrounding amino acid residues remained intact.

According to Gite and Shankar [3], the activity of the EDTA-treated S1 nuclease can be partially restored in the presence of Co^{2+} and Zn^{2+} ions. Our further studies will aim to expand this knowledge because it is still unclear whether any metal is capable of increasing (or inhibiting) the activity by replacing the natively present Zn^{2+} ions in the active site.

References

[1] T. Koval', L. H. Østergaard, J. Lehmbeck, *et al.* Structural and Catalytic Properties of S1 Nuclease from Aspergillus oryzae Responsible for Substrate Recognition, Cleavage, Non-Specifcity, and Inhibition. *PLoS ONE* **11**. DOI:10.1371/journal.pone.0168832. 2016.

[2] T. Koval', J. Dohnálek. Characteristics and application of S1-P1 nucleases in biotechnology and medicine. *Biotechnology Advances* **36(3)**, p. 603 - 612. DOI: 10.1016/j.biotechadv.2017.12.007. 2018.

[3] S. Gite, V. Shankar. Characterization of S1 nuclease. Involvement of carboxylate groups in metal binding. *European Journal of Biochemistry* **210(2)**, 437-441, 1992.

[4] W. A. Hendrickson. Anomalous diffraction in crystallographic phase evaluation. *Quarterly Reviews of Biophysics* **47(1)**, p. 49 - 93. DOI: 10.1017/S0033583514000018. 2014.

[5] U. Mueller, R. Förster, M. Hellmig, *et al.* The macromolecular crystallography beamlines at BESSY II of the Helmholtz Zentrum Berlin: Current status and perspectives. *The European Physical Journal Plus: EPJ Plus* **130**, p. 141/1 - 10. DOI: 10.1140/epjp/i2015-15141-2. 2015.

[6] W. Kabsch. XDS. *Acta Crystallographica Section D* **66(2)**, p. 125 - 132. DOI: 10.1107/S0907444909047337. 2010.

[7] P. R. Evans, G. N. Murshudov. How good are my data and what is the resolution? *Acta Crystallographica Section D* **69**, 1204-1214, 2013.

[8] A. J. McCoy, R. W. Grosse-Kunstleve, P. D. Adams, M. D. Winn, L. C. Storoni, R. J. Read. Phaser crystallographic software. *J. Appl. Cryst.* **40**, p. 658 - 674. DOI: 10.1107/S0021889807021206. 2007.

[9] H.M. Berman, J. Westbrook, Z. Feng, G. Gilliland, T.N. Bhat, H. Weissig, I.N. Shindyalov, P.E. Bourne. The Protein Data Bank. *Nucleic Acids Research* **28**, 235-242, 2000.

[10] G. N. Murshudov, P. Skubák, A. A. Lebedev, et al. REFMAC 5 for the refinement of macromolecular crystal structures. *Acta Crystallographica Section D* **67(4)**, p. 355 - 367. DOI: 10.1107/S0907444911001314. 2011.

[11] P. Emsley, B. Lohkamp, W. G. Scott, K. Cowtan. Features and Development of Coot. *Acta Crystallographica Section D* **66(4)**, p. 486 - 501. DOI: 10.1107/S0907444910007493. 2010.

[12] S. McNicholas, E. Potterton, K. S. Wilson, M. E. M. Noble. Presenting your structures: the CCP4mg molecular-graphics software. *Acta Crystallographica Section D* **67**, p. 386 - 394. DOI: 10.1107/S0907444911007281. 2011.

Acknowledgement

This work was supported by the MEYS CR (projects CAAS – CZ.02.1.01/0.0/0.0/16_019/0000778 and ELIBIO – CZ.02.1.01/0.0/0.0/15_003/0000447) from the ERDF fund, by the Czech Academy of Sciences (grant No. 86652036), and by the GA CTU in Prague (SGS22/114/OHK4/2T/14).

Table 1: Selected data collection statistics.
Values in parentheses represent the high resolution shell.

Dataset name	Cd-peak	Zn-low	Zn-peak
X-Ray Energy [eV]	6 600	9 630	9 680
Resolution Range [Å]	44.71 - 2.30 (2.38 - 2.30)	44.66 - 2.60 (2.72 - 2.60)	44.66 - 2.70 (2.83 - 2.70)
R_{meas}	0.155 (1.360)	0.373 (1.770)	0.324 (1.457)
$CC_{1/2}$	0.999 (0.709)	0.996 (0.746)	0.996 (0.785)
Mean I/σ(I)	18.3 (2.1)	10.4 (2.5)	10.8 (2.7)
Completeness [%]	99.4 (94.2)	100.0 (99.9)	100.0 (100.0)
Anom. Completeness [%]	99.2 (92.2)	100.0 (99.9)	100.0 (100.0)
Avg. Multiplicity	23.0 (13.5)	25.7 (25.9)	26.0 (25.1)
Avg. Anom. Multiplicity	11.9 (6.9)	13.7 (13.4)	13.9 (13.0)
Space group	$P2_12_12_1$		
Unit cell (a ; b ; c ; α)	63.19 ; 63.26 ; 118.86 ; 90.00		
Anomalous difference map maxima [σ]			
M 1	<2	<2	10.1
M 2	20.9	5.9	9.3
M 3	19.9	5.2	8.6